Impact of Contrast Functions in Fast-ICA on Twin ECG Separation

Mallika Keralapura, Mehrdad Pourfathi and Birsen Sirkeci-Mergen

***Abstract*—Fetal Electrocardiography (FECG) is a traditional method to measure fetal heart conduction signals during gestation. It can allow determination of fetal heart rate (FHR) along with amplitudes and timing of the FECG components, as these are indices for fetal health. FECG recording is problematic in the clinic due to the several interferences that corrupt the signal. It is recorded using simple electrodes placed on the mother's abdomen and is a part of this abdominal ECG. This abdominal ECG also contains several interferences. First the omnipresent maternal ECG (MECG) is a huge source of interference. Other possible noise sources are respiration and muscle activity along with thermal/electronic noise and noise from electrode-skin contact. The problem becomes all the more difficult and complicated for twin fetuses that could have FECG signals of similar morphology, amplitudes and heart rates. We are interested in extracting twin FECG signals from abdominal ECG using Independent Component Analysis (ICA) techniques, a way of Blind Source Separation (BSS). Twin fetuses require close monitoring of their heart health to track for congenital heart problems. These are especially important with identical twins complicated with twin-twin transfusion syndrome. In this paper, we work with the Fast-ICA technique and propose and test two types of data-centric contrast functions (*Poly-L* and *AbsPow*). These are obtained when the underlying data pdf is modeled as an exponential power distribution. We test this with 3 types of abdominal data sets - simulated, in-vivo (clinical) and ICA bench-marks with added Gaussian and muscle noise. We also compare performance across the standard fixed-point contrast functions in Fast-ICA using a normalized metric. We clearly show that *Poly-L* and *AbsPow* perform superior to the standard-ICA data-based *Pearson* method and works on par and in some cases better than standard ICA polynomial schemes like *Pow3*. When estimation was done over data acquisition time, it was clear that adequate data (10-30 mins) was needed for good performance. Performance metrics for data-centric contrast functions with order 3-4 (*Poly-3* and *AbsPow*) had the best performance for certain cases with little increase in complexity. This supports further testing with a large database of twin gestation data with heart defects.**

***Index Terms*—Fast-ICA, ECG, Twins, Contrast Functions**

I. Introduction

It is generally accepted that current methods of intra-uterine monitoring does not facilitate a comprehensive assessment of fetal well being [1]. One major indicator of fetal status is its cardiac function, to detect conditions like cardiac hypertrophy, arrhythmias and congenital heart defects [1]. Fetal cardiac monitoring becomes critical and complicated especially for identical twin gestations, as cardiac functional defects increases with such pregnancies [2]. Furthermore, this is more relevant nowadays, due to the frequent use of assisted reproductive technologies (like IVF) - that result in twins 40% of the time (both identical and non-identical). A 9-15 fold increase in cardiac function defects has been documented for identical twin pregnancies, and those complicated by twin-twin transfusion syndrome (TTTS) [2], over singleton pregnancies. In TTTS for instance, both fetuses are at risk for heart failure, and this condition requires simultaneous monitoring of the cardiac traces of both fetuses, to highlight signs of cardiac overload and dysfunction to optimize time of delivery [3].

Fetal cardiovascular status is diagnosed using ultrasound echocardiography. Ultrasound between 16 and 22 weeks gestation identifies 25-60% of major heart defects, but does not provide adequate information regarding the fetal cardiac conduction system [4]. Furthermore, ultrasound techniques require a trained technician/physician, frequent repositioning of the transducer and cannot be done in a home environment - something beneficial for problem pregnancies [5]. Fetal Electrocardiography (FECG) can be an attractive candidate to measure heart conduction signals and is obtained by means of ordinary electrodes placed on the mother's abdomen. It comprises of the standard ECG components (P, QRS and T waves). FECG could allow determination of the fetal heart rate (FHR) and other morphologic features of the recorded signal. Relative amplitudes and timing of the FECG waves (such as R-R interval, P/R, Q/R, S/R and T/QRS ratios) are indices for fetal health [1]. The R-R interval gives information of FHR and is useful to determine conditions like tachycardia (FHR$>$180bpm) or brachycardia (FHR$<$110 bpm) commonly seen with cardiac defects [6]. Fetal hypoxia could also be detected when P-R and R-R intervals are modified along with the depression of the ST segment [7].

FECG recording seems very attractive but its use in clinics have been limited due to the lack of clinical technology to display the signal. This is because FECG is a part of the abdominal ECG that also contains several interferences. Potential measurements on the mothers skin contain contributions from several bioelectric phenomena (maternal and fetal heart activity), potential distributions generated by respiration and stomach activity, and are affected by various kinds of noise (thermal noise, noise from electrode-skin contact, electronic noise, power-line interference) [8], [9]. Therefore, a highly sophisticated signal processing method is needed for FECG extraction and enhancement. The problem becomes all the more difficult in the case of twin fetuses that could have FECG signals of similar morphology, amplitudes and heart rates [3].

For singleton pregnancies, several signal separation algorithms have been proposed in the literature for separating

Manuscript received Jan 22, 2011; revised Jan 2011. This work was supported by College of Engineering, San Jose State University.

Dr. Keralapura is the director of the Biomedical Systems Lab in the Department of Electrical Engineering, San Jose State University. Mehrdad Pourfathi is a graduate student with interests in biological signal processing and Dr. Birsen Sirkeci is the director of the Communications Lab, Department of Electrical Engineering, San Jose State University. For correspondence, please contact Dr. Keralapura at Department of Electrical Engineering, One Washington Square, San Jose, CA 95192-0084. Tel/Fax: (408) 924-3915/3925. Email: mallika.keralapura@sjsu.edu. Authors have contributed equally to the work.

FECG from abdominal ECG [7]. Classical filtering methods and adaptive techniques like the least means square (LMS) adaptive filtering technique [10], IIR adaptive filtering [11], singular value decomposition techniques [12] and wavelet transform [13] based methods are examples that have been proposed. More recently, blind source separation (BSS) techniques [8], [14] have also been designed. The main advantage of BSS techniques is that they do not require any a priori knowledge about the signals (contrary to filtering methods). For example, Gupta *et. al.* [9] did a comparative study of 4-channel adaptive MECG-FECG cancellers and BSS methods and found BSS methods to be superior for extraction and enhancement of fetal ECG. BSS methods use principal component analysis (PCA), singular value decomposition (SVD) or independent component analysis (ICA) techniques. Independent component analysis (ICA), uses higher order statistics to decompose the signal into statistical independent components. Using this framework, Ye *et. al.* [15] developed an adaptive ICA algorithm to separate mixtures of sub-gaussian, super-gaussian, and nearly gaussian signals. They tested their algorithm on singleton abdominal ECG signals and reported superior performance when compared to the standard ICA schemes.

Only a few studies have been reported for twin gestations using ICA. For example, Lathauwer *et. al.* [8] used online abdominal data of twins to develop the concept of MECG and FECG subspaces. Taylor *et. al.* [16] is probably the only comprehensive clinical study on both single and twin gestations with the aim of documenting the duration of fetal cardiac time intervals in uncomplicated pregnancies. The focus was purely on the clinical aspects and they use a clinically patented signal processing technique that was based on the ICA. They test this on a population of 250 singleton and 58 twin pregnancies between 15 to 41 weeks of gestation. For singleton pregnancies, the main outcome was duration of FECG time intervals as a function of gestational age. P-R and QRS intervals were the only parameters that increased significantly with gestational age. For singletons, a signal separation success rate of 85% (213/250) was reported that was significantly poorer between 27-36 weeks gestation. In twins and triplets, separate FECGs were obtained in 78% of the signals. Studies reported by Comani *et. al.* and Burghoff *et. al.* [3], [17] measured and separated twin magnetocardiography data (an bio-magnetic approach to measuring fetal cardiac conduction) for diagnosis. Burghoff *et. al.* applied the ICA algorithm-TDSEP to 9 magnetocardiograph datasets of twin pregnancies acquired between the 28th and 38th week of pregnancy. The results showed that the maternal and fetal components could be separated not only from each other but also from sources of noise and artifacts. This study demonstrates the use of magnetic signals beyond 27^{th} week gestation where bioelectric FECG begins to fail.

In additional to separating FECG from singleton or twin pregnancies, standard ICA algorithms like INFOMAX [18], the JADE, the FastICA and the MERMAID [19], [20] have been applied to ECG for various other purposes like artifact and noise removal and analysis of the autonomic control of the heart [7]. In the ICA domain itself, several estimation methods have been proposed. The two methods most widely used in practice are the fixed-point algorithm and the maximum likelihood stochastic gradient algorithm [20]. In fixed point algorithms, the criterion function includes a fixed non-linearity and there is an implicit assumption about the model for source (maternal or fetal) distributions. In maximum likelihood estimation, source distributions are modeled explicitly using large parametric families of distributions with free parameters to estimate, like the Pearson system [21].

The objective of this work is to investigate the FastICA algorithm using fixed point schemes and compare these with our two newly developed data-centric alternatives - polynomial-based and exponential-based contrast functions in the context of twin FECG extraction from in-vivo abdominal ECG channel data. This work improves upon our previous work [22] that used only polynomial schemes with simulated data. In this work, the data is initially simulated with different types of interference for feasibility testing, but the focus is on processing the in-vivo data available online with these new techniques. We reconstruct the twin FECG signals and analyze the errors using a normalized metric.

Notations: In this paper, we adopt the following notations. The lower case letter denotes a scalar, the boldface lower case letter denotes a vector, boldface upper case letter denotes a matrix. The symbol R^+ denotes the positive real numbers. The derivative of the function $f(y)$ is denoted as $f'(y)$. The $\mathbf{x}^T$ denotes the transpose of the vector $\mathbf{x}$. The $E\{y\}$ denotes the expected value of the random variable y. The $\log$ denotes the natural logarithm function.

II. Independent Component Analysis

Imagine the abdominal ECG recordings of a pregnant woman carrying twins are denoted as $x_1(t), x_2(t)$ and $x_3(t)$, where x_i, $i = 1 \dots 3$ are the amplitudes and t is the time index. It is common to model these abdominal ECG recordings as a weighted sum of the twin fetal and maternal signals, which we denote by $s_1(t), s_2(t)$, and $s_3(t)$ [7]. This linear relationship could be expressed as

$$x_1(t) = a_{11}s_1(t) + a_{12}s_2(t) + a_{13}s_3(t) \quad (1)$$

$$x_2(t) = a_{21}s_1(t) + a_{22}s_2(t) + a_{23}s_3(t) \quad (2)$$

$$x_3(t) = a_{31}s_1(t) + a_{32}s_2(t) + a_{33}s_3(t) \quad (3)$$

In the above set of equations (1-3), if the mixing coefficients are known, we can find the source estimates $\hat{s}_1(t), \hat{s}_2(t), \hat{s}_3(t)$ by either using least squares or by simply inverting the linear system. However, in our context neither mixing coefficients nor the source signals are known. A blind source separation method, ICA (Independent Component Analysis) [20] uses the assumption of statistical independence among source signals to estimate the source signals and the mixing coefficients. It does not require the knowledge of mixing coefficients and the statistical independence assumption is not unrealistic in the case of separation of maternal and fetal ECG signals.

It is usually more convenient to use vector-matrix relations instead of linear equations (1-3). In general terms, N linearly mixed sources can be represented in the vector form as

$$\mathbf{x}(t) = \mathbf{A}\mathbf{s}(t), \quad (4)$$

where $\mathbf{s}(t) = [s_1(t)s_2(t) \dots s_N(t)]^T \in \mathcal{R}^N$ denotes the N source signals, $\mathbf{x}(t) = [x_1(t)x_2(t) \dots x_M(t)]^T \in \mathcal{R}^M$ denotes the observation vector, and $\mathbf{A} \in \mathcal{R}^{M \times N}$ is formed

from coefficients a_{ij}, $i = 1 \dots M, j = 1 \dots N$. In our set-up, the sources could include not only the fetal and maternal signals but also various noise components such as white Gaussian noise and electromyogram (EMG) noise from the abdominal muscle. In ICA, it is assumed that the observed signals are at least as many as the sources ($M \geq N$).

ICA methods try to determine the de-mixing matrix $\mathbf{W}$, which is the inverse of $\mathbf{A}$, so that the rows of $\hat{\mathbf{s}}(t) = \mathbf{W}\mathbf{x}(t)$ becomes statistically independent. There are various measures of statistical independence in literature such as mutual information and non-gaussianity [20]. In this work, we focus on ICA algorithms using maximization of non-gaussianity. The relation between non-gaussianity and independence could be explained easily using the central limit theorem (CLT) [23]. According to the CLT, the distribution of a sum of independent random variables tends to a Gaussian distribution under certain assumptions. This implies that the sum tends to be "more" Gaussian than the original random variables. Notice that multiplication with $\mathbf{W}$ (inverse of mixing matrix $\mathbf{A}$) is also a linear operation. Consider a single row of $\hat{\mathbf{s}}(t) = \mathbf{W}\mathbf{x}(t)$, e.g.

$$\hat{s}_i(t) = \mathbf{w}^T\mathbf{x}(t) = \mathbf{w}^T\mathbf{A}\mathbf{s}(t) = \mathbf{z}^T\mathbf{s}(t), \tag{5}$$

where $\mathbf{w}$ is the i^{th} row of $\mathbf{W}$, and $\mathbf{z} = \mathbf{w}^T\mathbf{A}$. Eqn. 5 tells that each source estimate can be represented as linear combination of the original sources. Since original sources are assumed to be independent, if we find a $\mathbf{w}$ so that $\hat{s}_i(t)$ is "least" Gaussian, then our estimate is closest to the original source. Hence, in the ICA context, independence is equivalent to non-gaussianity.

In the literature, two different measures of non-gaussianity are kurtosis and negentropy [20]. The kurtosis of a random variable y is defined as

$$\mathcal{K}(y) = E\{y^4\} - 3(E\{y^2\})^2 \tag{6}$$

For a zero-mean Gaussian random variable, the kurtosis is known to be zero. If the kurtosis is away from zero, the random variable could be considered to be non-Gaussian. In theory, kurtosis is the optimized criterion for ICA, however, in practice since the value is estimated from the measured samples (since underlying a probability density function (pdf), is unknown), ICA based on kurtosis could be sensitive to outliers [20], [24].

On the other hand, the negentropy for a random variable y is defined as

$$J(y) = H(y_{gauss}) - H(y), \tag{7}$$

where $H(y) = \int f(y) \log f(y) dy$ denotes the information theoretic differential entropy, and y_{gauss} is a Gaussian random variable with the same covariance as y. Since a Gaussian random variable has the largest entropy among all the random variables with the same variance, the negentropy is always nonnegative. The larger the negentropy, the closer the random variable gets to be non-Gaussian. Similar to kurtosis, the main issue with negentropy calculations is the fact that the distribution of the random variable y is needed in the calculation. Instead, we can use approximation of negentropy [20]. The classical method of approximating negentropy using higher-order moments [20] will give

$$J(y) \approx \frac{1}{12} E\{y^3\}^2 + \frac{1}{48} \mathcal{K}(y)^2 \tag{8}$$

TABLE I
FAST-ICA ALGORITHM

1. Make the data zero-mean (centering)
2. Whiten the data
3. Choose and initial random vector $\mathbf{w}$. The vector $\mathbf{w}$ denotes one column of the estimated inverse matrix $\mathbf{W}$.
4. Fixed-point iteration:
   $\mathbf{w} \leftarrow E\{\mathbf{z}g(\mathbf{w}^T\mathbf{z})\} - E\{g'(\mathbf{w}^T\mathbf{z})\}\mathbf{w}$
   where $\mathbf{z}$ is the whitened & centered data, and $g()$ is the derivative of the contrast function $G()$, and $g'()$ is its second derivative.
5. Normalization: $\mathbf{w} \leftarrow \mathbf{w}/\|\mathbf{w}\|$
6. Check convergence, if not go to step-4.

Similar to kurtosis, this form of approximation is not a robust measure for nongaussianity. Instead, we can use another approximation of negentropy [20], Eqn. 9,

$$J(y) \approx [E\{G(y)\} - E\{G(\nu)\}]^2 \tag{9}$$

for a non-quadratic function G, and zero-mean, unit variance Gaussian random variable ν. The nonlinear function G is known as *contrast function*. Ideally, if the source distribution $f(y)$ is known, then $G(y) = -logf(y) = -\int \frac{f'(y)}{f(y)} dy$ would be the optimal choice for the contrast function.

We have discussed the ICA method as an optimization problem in which the objective function negentropy (Eqn. 7) or its approximations (Eqn. 9) are maximized. In the literature, there are works which have used other objective functions such as the likelihood [25] or the mutual information [26], [27] for source separation purposes. The performance of the ICA method depends on the choice of objective function. On the other hand, another component of ICA method is the algorithm used for implementation of the optimization problem, which determines the speed of the ICA method. Gradient based optimization algorithms such as Newton's method or stochastic gradient descent lead to slow convergence rate. In this work, we focus on the fast-ICA algorithm [19] which is faster than the gradient based methods. The details are given below.

A. Fast-ICA Algorithm

Fast-ICA is a fixed point algorithm that maximizes an approximation of negentropy for non-gaussianity. The details of the fast-ICA algorithm are shown in Table II-A. The main iteration step in the algorithm is

$$\mathbf{w} \leftarrow E\{\mathbf{z}g(\mathbf{w}^T\mathbf{z})\} - E\{g'(\mathbf{w}^T\mathbf{z})\}\mathbf{w}.$$

Here the vector $\mathbf{w}$ denotes one column of the estimated inverse matrix $\mathbf{W}$ (inverse of the mixing matrix $\mathbf{A}$). The vector $\mathbf{z}$ is the whitened & centered data, $g()$ is the derivative of the contrast function $G()$, and $g'()$ is its second derivative. Commonly used contrast functions with Fast-ICA algorithm are below listed as:

- *Skew:* $g(y) = y^2$
- *Pow3:* $g(y) = y^3$
- *Gauss:* $g(y) = y\ exp(-y^2/2)$
- *Tanh:* $g(y) = tanh(y)$

Main advantages of the fast-ICA algorithm are its speed (superior to gradient-based schemes), user-friendliness (does not require the probability distribution or selection of certain parameters), and its flexibility for performance optimization (done via choice of the contrast function $G(y)$ or equivalently $g(y) = G'(y)$).

B. Practical Contrast Functions

Practically, for any non-quadratic contrast function G, the negentropy approximation in Eqn. 9 is valid and ICA will separate the sources. However, if one needs to optimize the performance, choice of contrast function becomes important. In general, the selection of the contrast function depends on the data and the application. For example, if the data seems to have outliers, one should choose contrast functions that are more robust. On the other hand, speed/complexity of algorithm could be another concern.

If we choose $G(y) = y^4$ (for symmetric distribution of y) in Eqn. 9, we obtain the kurtosis-based approximation, Eqn. 8 which also might suffer from robustness. In particular, by choosing G that does not grow too fast, one can obtain more robust estimators. The following choices of G have proved to be useful and robust contrast functions [20]:

$$G(y) = \frac{1}{a_1} \log \cosh a_1 y, \quad (Tanh)$$

$$G(y) = -\exp(-y^2/2), \quad (Gauss)$$

where $1 \leq a_1 \leq 2$ is some suitable constant.

In the literature, optimization of contrast function for different data sets is a recent popular topic. In [28], the authors use $G(y) = \log(1+y^2/2), g(y) = G'(y) = y/(1+y^2/2)$ for image extraction. The proposed function has similar statistical behavior as $Tanh$, but runs faster (lower computational complexity) and results in better quality image extraction for supergaussian sources. In [29], the authors use a modified Gaussian function $G(y) = exp(-y^2/(2K^2))$ where K is a parameter that measures the spread of the distribution. The modified Gaussian function outperforms both $Tanh$ and $Gauss$ methods with the selection of K through experiments. In [30], the authors use

$$g(y) = G'(y) = \frac{x-a}{b_0 + b_1 x + b_2 x^2} \quad (Pearson) \qquad (10)$$

as the derivative of the contrast function. Here the parameters a, b_0, b_1, b_2 are found using the method of moments. It is worth mentioning that the Pearson system uses some statistical properties of the data to calculate constants a, b_0, b_1, b_2 in the contrast function.

It is known that any non-quadratic function G can be used to perform ICA [20, Theorem 8.1]. In particular, by choosing a G that does not grow too fast, one can obtain robust estimators to outliers. In Fig. 1, we plot the behavior of each contrast function around zero. However, assuming the data does not contain any outliers, the choice of the contrast function is highly dependent on the data if one wants to optimize the performance.

In the next section, we describe new methods that uses certain characteristics of the ECG signal to derive data-centric contrast functions.

C. Empirical density based Fast-ICA for ECG

In this section, we propose a new way of obtaining the contrast function using an estimate of the underlying probability density function (pdf) of the sources (maternal and twin fetal). This way, certain properties of the source signals can be incorporated into the Fast-ICA algorithm. It is important to note that the mother ECG, the twin fetal ECG, and the noise signals have different morphological and temporal characteristics, and utilizing the same contrast function could result in suboptimal solutions. Our goal is to incorporate the differences in the source signals into the Fast-ICA by utilizing different contrast functions that are functions of the empirical pdf.

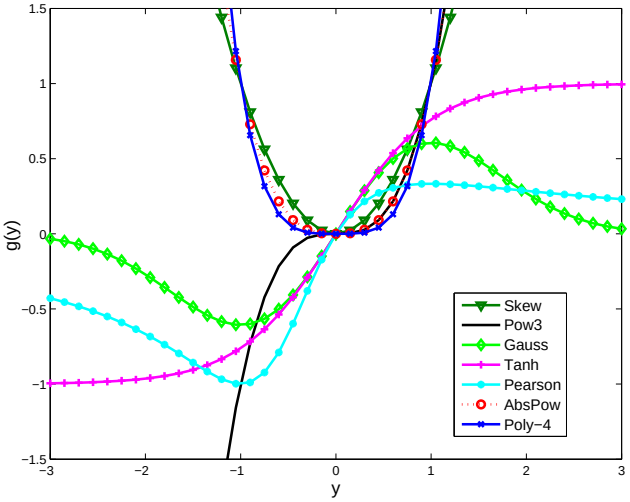

Fig. 1. The behavior of contrast functions around zero. *Pearson* is plotted for parameters $a = 0, b_0 = b_1 = b_2 = 1$ and *AbsPow* is plotted for $\alpha = 3$.

We follow the following steps in order to obtain contrast functions that are data centric.

1) *Generate template source signal*: More details are provided in the next section.
2) *Obtain the empirical pdf*: Among the various ways of obtaining pdf estimates, we choose 3 techniques - scaling the histogram of the observed data, the kernel density estimation (kde), which is a non-parametric method, and parametric density estimation for exponential power family distributions
3) *O*btain the contrast function: we set the contrast function as the score function: $G(y) = -\log(f_e(y))$, where $f_e(y)$ is the empirical pdf for the selected source. Note that if the pdf estimation was perfect, then this would be the optimal choice for the contrast function.

In the Fast-ICA algorithm, the first and the second derivatives of the contrast function $G(y)$ are needed. To obtain these from the pdf, we propose to fit a polynomial to $G(y)$ and then take the first and second derivatives analytically. This is so-called *Poly-L* scheme. In this case of polynomial fit with a fixed order, the contrast function would be

$$G(y) = -log(f_e(y)) \approx \sum_{i=0}^{L+1} a_i y^i \qquad (11)$$

$$g(y) = G'(y) = \sum_{i=0}^{L} a_{i+1}(i+1) y^{i-1} \quad (PolyL) \qquad (12)$$

The coefficient a_0 could be selected to be zero for simplicity. The polynomial order could also be optimized for different sources. Note that the standard Fast-ICA offers polynomial based contrast functions *skew* and *pow3* but with unoptimized coefficients.

In the scenario, where we utilize parametric density estimation for exponential power family distributions, that is

$p(y) = c_1 exp(-c_2|y|^\alpha)$, the contrast function reduces to

$$G(y) = -log(c_1) + c_2|y|^\alpha. \quad (AbsPow) \qquad (13)$$

We call this contrast function *AbsPow* due to its similarity to standard *Pow3* contrast function. This method is not totally un-explored. In [19], it was suggested that the exponent α should be chosen to be less than 2 for robustness. In [31], authors use this in another context: separation of electro-gastrogram signal from artifacts such as gaussian noise. In this case, the parameters c_1, c_2 and α were obtained using a quasi-Newton method. The contrast functions proposed in both works [19], [31] are suboptimal in this context of ECG signal extraction.

As a novel contribution, we have experimentally optimized *AbsPow* contrast function for twin-ECG signal extraction. We concluded that the parameters $c_1 = 1, c_2 = 1, \alpha = 3$ performs quite well. Hence, we adapt $G(y) = |y|^3$ as our *AbsPow* contrast function in the simulation section.

D. Data Sets

We explore our data-centric techniques and compare with other Fast-ICA schemes using a combination of simulated data using the techniques described by [32], real in-vivo data from an online database (DaISy, [33]) and a standard ICA database (ABio7, [34]), a bench-mark of ICALAB.

1. Simulated Data: We generate all the simulated ECG source signals (maternal and twin fetal) based on a dynamical model presented in [32]. The dynamical model is based on three coupled ordinary differential equations which is capable of generating realistic synthetic electrocardiogram (ECG) signals. The operator can specify the mean and standard deviation of the heart rate along with the morphology of the PQRST cycle. The model generates a trajectory in a three-dimensional (3-D) statespace with coordinates (x,y,z). Each revolution on this circle corresponds to one RR-interval or heartbeat. Distinct points on the ECG, such as the P, Q, R, S, and T are described by events corresponding to negative and positive attractors/repellors in that direction. These events are placed at fixed angles along the unit circle given by θ_i. The resultant ECG signal is synthesized by solving a set of differential equations shown below:

$$\begin{aligned} \dot{x} &= \alpha x - \omega y; \qquad \dot{y} = \alpha y + \omega x \\ \dot{z} &= -\sum_{i\epsilon(PQRST)} a_i \Delta\theta_i exp\left(\frac{-\Delta\theta_i{}^2}{2b_i{}^2}\right) - (z - z_0), \end{aligned} \qquad (14)$$

where $\alpha = 1 - \sqrt{(x^2 + y^2)}$, $\Delta\theta_i = (\theta - \theta_i) mod 2\pi$, $\theta = atan2(x, y)$, $z_0 = Asin(2\pi f_2 t)$ and f_2 is the respiratory frequency.

Visual analysis of a section of typical ECG from a normal subject was used to suggest suitable times, and, therefore, angles (θ_i) and values of a_i and b_i for the PQRST points. Some further fine-tuning was done to these parameters to find suitable values for a_i, b_i and $\Delta\theta_i$, for each segment to represent more realistic maternal and fetal ECG signals with amplitudes, timing and frequency content close to clinically reported signals. Table II lists the values used into the ECG model and Table III shows the range of ECG amplitudes and timing values used in this paper. These values fall within the range reported by Shepovalnikov *et. al.* [35] and [16] for in-vivo maternal and twin fetal ECGs.

TABLE II
PARAMETERS INPUT INTO THE ECG MODEL

MECG	P	Q	R	S	T
time (s)	-0.202	-0.044	0	0.044	0.216
a_i;b_i	0.3;0.19	0.3;0.1	28;0.08	-7;0.1	0.5;0.29
θ_i(deg)	-80.47	-16.94	0	16.94	84.71
FECG1;2	P	Q	R	S	T
time (s)	-0.084;-0.088	-0.02;-0.024	0;0	0.02;0.024	0.056;0.076
a_i	0.04;0.04	-3;-2	3.5;3	-4;-5	0.1;0.2
b_i	0.5;0.4	0.3;0.32	0.3;0.33	0.2;0.22	0.5;0.4
θ_i(deg)	-103.5;-116.31	-31.5;-42.46	0;0	31.5;42.46	72;95.08

TABLE III
DURATIONS AND AMPLITUDES OF MECG AND FECG

MECG	$P-Q$	$Q-T$	$R-R$	$S-T$	QRS
(sec)	0.158	0.26	0.83	0.172	0.088
FECG1;FECG2	$P-Q$	$Q-T$	$R-R$	$S-T$	QRS
(sec)	0.064;0.064	0.076;0.1	0.4;0.39	0.036;0.09	0.04;0.048
MECG	P	Q	R	S	T
(mV)	0.521	0.15	2.102	-0.266	0.804
FECG1;FECG2	P	Q	R	S	T
(mV)	0.135;0.133	0.053;0.077	0.242;0.231	0.089;0.058	0.142;0.141

Fig 2 shows an example of the maternal and twin fetal ECG data generated using the ECG dynamical model [32] and parameters in Table II. The figure shows that the 2 ECG signals are different in terms of their morphological and temporal behavior as described in Taylor *et. al.* [16] and Shepovalnikov *et. al.* [35]. Note that the FECG waveform is significantly smaller in amplitude when compared to the MECG waveform. We also show a normalized pdf estimated using standard histograms and the KDE method for long length (10-15 minutes) MECG and FECG simulated data. The length of the data matrix is chosen such that the pdf shape converges. This pdf will be used for the design of the data-centric methods we have described. We also estimated the power spectral density using the standard Welch technique and calculated the center of gravity of the spectrums. Values obtained for MECG, FECG1 and FECG2 were 9.27Hz, 20.22Hz and 17.59Hz. These values closely agree with those reported in [35].

2. Real In-vivo Data: We first used the DaISy database [33] that comprises of cutaneous potential recordings of a woman with a singleton pregnancy with 8 channels of data available. Channels 1-5 are abdominal channels and channels 6-8 are thoracic channels. The electrocardiogram measurements are recorded over 10 s, and sampled at 250 Hz. Twin pregnancy data is not available on any source online and requires a separate clinical study to obtain it. We still use this singleton pregnancy data and add on another simulated fetal data set and then test our new approaches. This technique of adding on data to the online data set has been reported in [8] due to the unavailability of twin data. To do this properly - first we separated the mother and single fetus from the DaISy data-set after base-line correction using an independent ICA technique (not the FAST-ICA tools) such as the JADE-ICA [20]. Jade-ICA algorithm, like other ICA methods, relies on statistical independence of the sources. JADE has been used in the context of separating

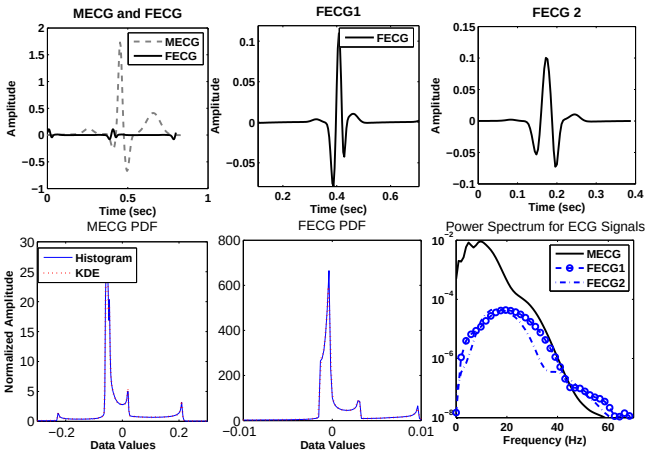

Fig. 2. Simulated maternal and twin fetal ECG signals using parameters and values from Table II and III along with pdfs and power spectral densities of the signals

fetal data from singleton pregnancies [20]. One we separate the signals, we then simulate a second FECG with similar heart rate ($\pm$10 bpm) and morphology using the techniques discussed in the above simulated data section. The ability to reconstruct this added fetal signal is then tested among the different techniques. Fig 3 shows the original in-vivo data from the online database. Fig 4 shows the separated MECG and FECG1 data using JADE-ICA along with the simulated FECG2 data and noises used for the simulations.

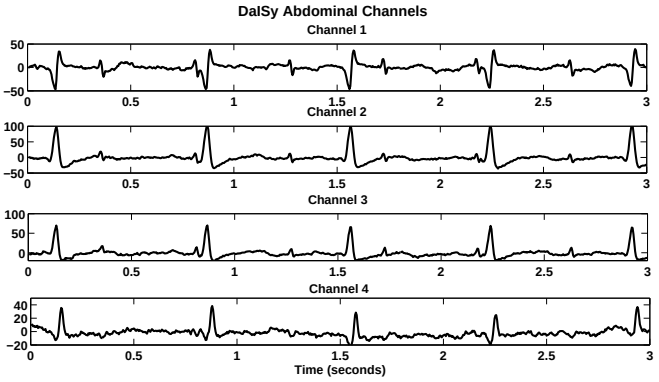

Fig. 3. Original DaISy database abdominal channels for a singleton pregnancy.

3. ICA database - ABio7: The ABio7 data-set is a benchmark in ICALAB [34] and consists of 7 channels. Each signal had 5000 samples, 250 Hz sampling rate with zero means and unit variances. Three signals s1, s5, and s6 are sub-Gaussian, two signals s4 and s7 are super-Gaussian, and the others s2 and s3 were Gaussian noise. The data is shown in Fig 5.

E. Simulation Studies

Several studies were conducted on the 3 data-sets described above to compare the performance of data-centric *Poly-L and* AbsPow schemes to other Fast-ICA implementations. For simulated data, when 5 sources were used (MECG, 2 FECGs and 2 noise sources), a 5-by-5 randomly generated mixing matrix was used to give a set of linearly mixed vectors of the sources. The same procedure was used for

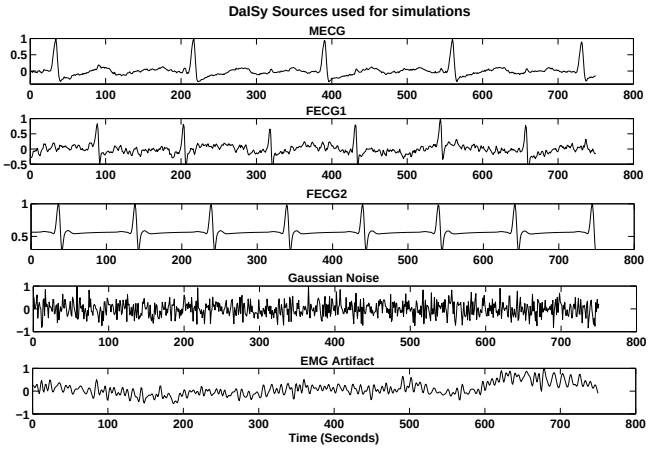

Fig. 4. Separated MECG and FECG1 data from the DaISy used JADE-ICA, simulated FECG2 data, Gaussian and EMG noise used for simulations.

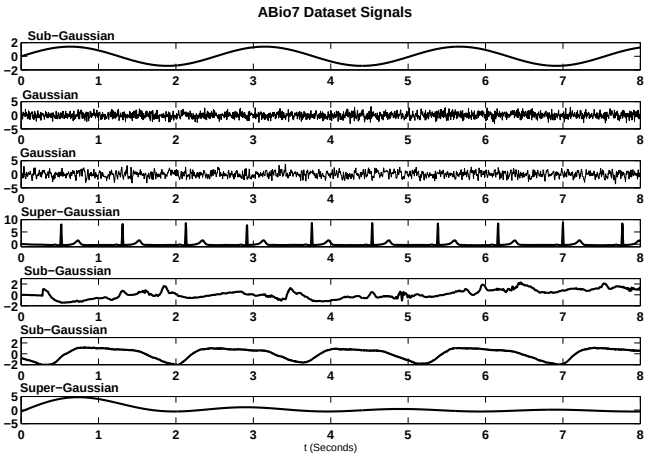

Fig. 5. Illustration of the ABio7 data-set with sub-gaussian, super-gaussian and gaussian signals

in-vivo maternal data with added simulated fetal ECGs. For the DaISy dataset, baseline wander was first removed using a bi-directional low pass filter from [36] prior to mixing. For all cases, 100 simulations were run and PI metric was averaged over all trials.

We then quantitatively compared the reconstruction performance using a metric called the performance index or the PI-metric. Since ICA methods cannot exactly determine the scaling (the energy) of the sources, and their orders, the Amari distance [20] is useful for performance comparison. The Amari distance (or the PI metric) is defined as follows: Let e_{ij} be the (i,j) th element of the matrix $\mathbf{E} = \mathbf{WA}$. Then the PI metric is -

$$PI = \frac{1}{n}\sum_{i=1}^{n}\left\{\left(\sum_{k=1}^{n}\frac{|e_{ik}|}{max_j|e_{ij}|}-1\right)+\left(\sum_{k=1}^{n}\frac{|e_{ki}|}{max_j|e_{ji}|}-1\right)\right\}. \quad (15)$$

We explored the variation of the PI metric, that measures reconstruction quality, over the data-centric and standard ICA schemes. We do this over time, to see the dependence of the quality on acquisition time, and also over fetal heart rate changes. Below is a list of the simulations we run and report in this paper.

1) PI metric over data acquisition time for simulated data (MECG=72 bpm, FECG1=150 bpm, FECG2=147 bpm) corrupted with Gaussian noise (zero mean, unit variance) and electromyographic (EMG) artifact. Gaussian noise is chosen to simulate the collection of the numerous sources of noise all added up together including electrode noise, environmental noise, electronics, etc. The EMG signal arises from the mother's abdominal muscle movements (collected from physionet online signal archives [37]).
2) PI metric for fixed time (400 s) for simulated data (MECG=72 bpm, FECG1=150 bpm) but varying FECG2 between 143 and 157 bpm again corrupted with Gaussian noise and electromyographic (EMG) artifact.
3) PI metric over time and over fetal heart rate changes for all schemes for real in-vivo MECG and simulated FECGs.
4) PI metric for the DaISy database across all schemes and over FECG2 heart rates.
5) PI metric for various schemes in their ability to extract sub-gaussian, gaussian and super-gaussian signals from the ABIO7 dataset [34].

III. Results and Discussion

The first simulation we ran was on simulated data to compare all the ICA schemes. In Fig 6, we first notice a decrease in the PI metric over data acquisition time indicating that long-time data should be acquired and used for ICA estimation. Another interesting observation we made, was the clustering in the performance of *Poly-3*, *AbsPow* and the standard ICA *Pow3*. Of these three, *Poly-3* and *AbsPow* was newly proposed by us in this paper. This indicates that the new techniques perform on-par or sometimes better than the standard *Pow3*. Interestingly, a reason why their performance could be similar is that they all stem from exponential power family data distributions of similar orders. To illustrate this point, *Poly-3* is the contrast function when the source pdf is modeled as $f(y) \propto exp(\sum_{i=0}^{4} a_i y^i)$, *AbsPow* is obtained when pdf is modeled as $f(y) \propto exp(|y|^3)$ and *Pow3* is obtained when source pdf is modeled as $f(y) \propto exp(y^4)$. Other fixed-point schemes like *Gauss* and *Tanh* do not use the data in their estimation but seem to perform on-par with the data-centric schemes. The performance of the data-centric schemes show improvement with in-vivo MECG data, seen in Fig 7. In this case we use abdominal MECG from the online physionet database [37] and combine simulated twin FECG using the description in Sec. II-D. Both *AbsPow* and *Poly-3* show best performance compared to all other schemes for maximum acquisition time of 2000s. In particular, in both examples it was significantly better than the already established data-centric scheme - *Pearson* which is known to superior in modeling distributions that are close to Gaussian, but fails otherwise [1]. The improvement in performance could be due to the fact that exponential power distributions of order $3-4$, models real ECG data more effectively. In these results, the standard deviations of the PI metric was relatively constant over acquisition time.

[1] In [30], it is suggested that the Pearson contrast function is replaced with Tanh if the kurtosis of the data greatly differs of the kurtosis of Gaussian distribution. For fair comparison with Tanh, we did not implement this suggestion.

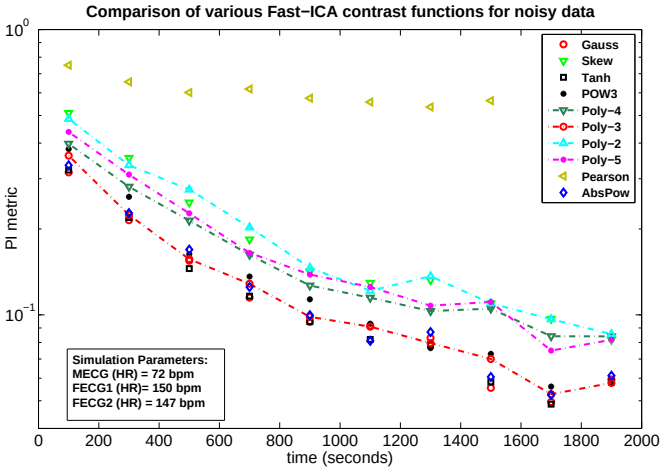

Fig. 6. PI metric over time for the data-centric schemes (Poly-L) and AbsPow compared with standard Fast-ICA schemes for simulated data with added Gaussian noise and EMG artifact.

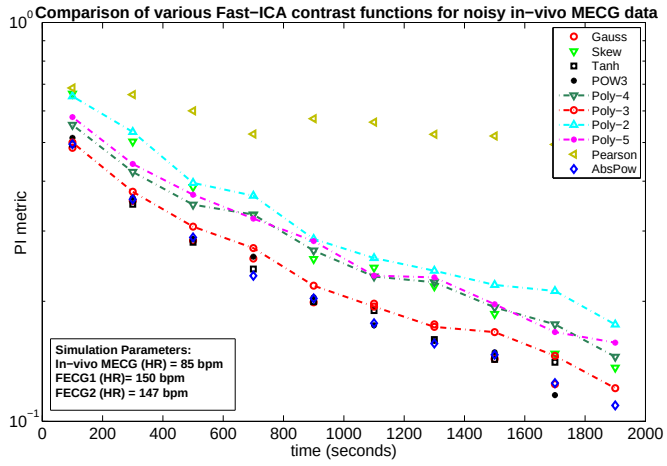

Fig. 7. PI metric over time for the data-centric schemes (Poly-L) and AbsPow compared with standard Fast-ICA schemes for in-vivo MECG and simulated FECGs with added Gaussian noise and EMG artifact.

We also investigated the role of heart rate difference between the 2 fetal signals on the performance of the ICA over different schemes, shown in Fig 8. As expected, the performance is significantly worse when the heart rates are identical - as the ICA scheme does not recognize the signals being separate. This is in-spite of the signals having different amplitudes. We see the same type of clustering in our newly designed exponential power family based contrast functions (*AbsPow*, *Poly-3*) with standard *Pow3*. The performance of *AbsPow* improves over the rest of the schemes when in-vivo MECG data was used, as seen in Fig 9, again indicating that real ECG data is better modeled with an exponential power distribution - $f(y) \propto exp(|y|^3)$. The performance metric for variation over heart rate for all schemes shifts upwards when FECG heart rates are higher (around 180 bpm) [22]. This has implications when trying to separate twin data that experience tachycardia (high heart rates). This indicates that such ICA schemes may need to re-optimized for not only the data but also features like the heart rate.

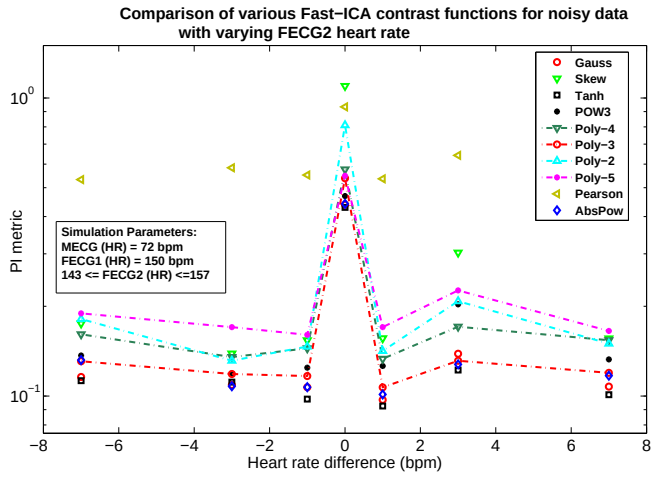

Fig. 8. PI metric for the data-centric schemes (Poly-L) and AbsPow compared with standard Fast-ICA schemes for varying FECG2 heart rate with added gaussian and EMG artifact.

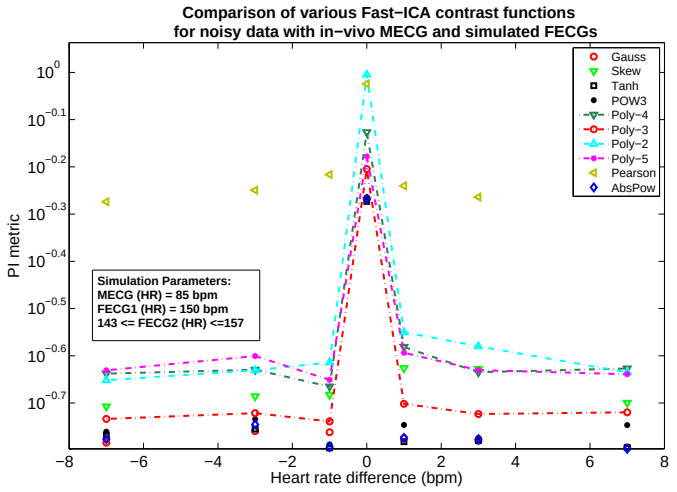

Fig. 9. PI metric for the data-centric schemes (Poly-L) and AbsPow compared with standard Fast-ICA schemes for in-vivo MECG and simulated FECGs and varying FECG2 heart rate with added gaussian and EMG artifact.

The same heart rate difference test was then applied to the in-vivo DaISy database. This database has data from a singleton pregnancy and the raw channel data is shown in Fig 3. The raw channel data was separated using JADE-ICA first to isolate the sources of MECG and one FECG. Another FECG was added on in this with similar morphology and heart rates. The source data for DaISy is given in Fig 4. We see different trends for this data-set as shown in Fig 11. We do not see any variation over heart rate difference. Reasons being: first, given that the FECG2 was simulated and FECG1 was real in-vivo data, they cannot be absolutely identical, even though we tried to make them as close as possible. ICA is really sensitive to even minute changes and can separate all the signals effectively even when the 2 signals have the same heart rate. The *AbsPow* performed the best among the exponential power distributions but was slightly worse than the standard Gauss and Tanh functions. *Poly-3* was not too far behind in its performance when compared to *AbsPow*. This change in performance could be due to the mix of simulated and real fetal data. Its performance could improve if real twin data was used. The reconstructed signals for this database are shown in Fig 10 which clearly demonstrates the similarity to the actual source signals used (Fig 4). In this case, the standard deviation of the PI metric was relatively constant over acquisition time for all ICA schemes except *Pearson* and *Poly-5* - both showed higher variability.

When we added Gaussian noise and EMG artifact to this data-set, the performance of all the schemes degraded except *Pearson* and *Poly-4* (see Fig. 12). *AbsPow* got significantly worse but *Poly-3* was still able to separate the signals out quite well. *Pow3* performance was robust to noise. The standard non-data centric schemes performed better in this case because of the high noise. Noise in the data will significantly effect the modeling of the data-pdf causing the data-centric methods to perform worse than the standard fixed-point schemes that do not use the data directly.

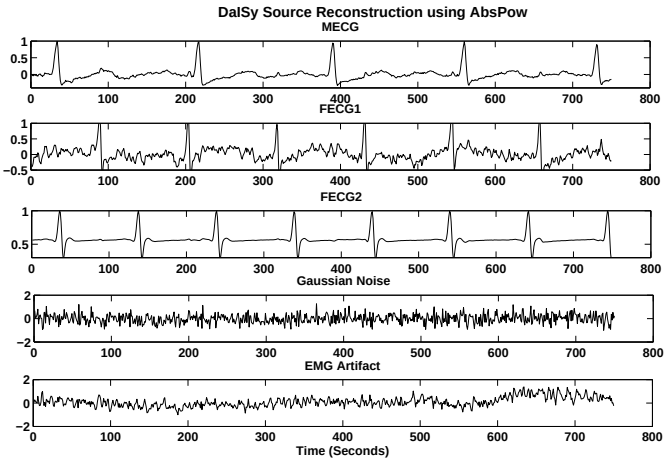

Fig. 10. Reconstruction of the DaISy source signals using data-centric AbsPow.

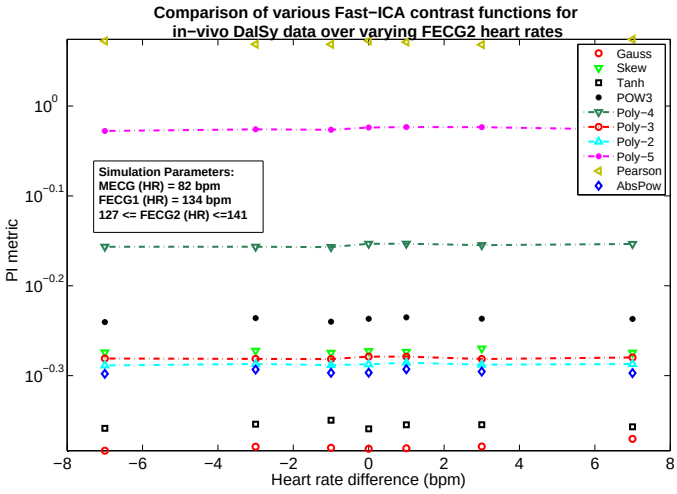

Fig. 11. PI metric for the data-centric schemes (Poly-L) and AbsPow compared with standard Fast-ICA schemes for in-vivo DaISy data-base with varying FECG2 heart rate and no noise added.

The last test was on the ICALAB bench-mark database ABio7. This is a difficult data-set to separate effectively as the set contains sub-, super- and purely gaussian signals. Among the exponential-based contrast methods, our data-

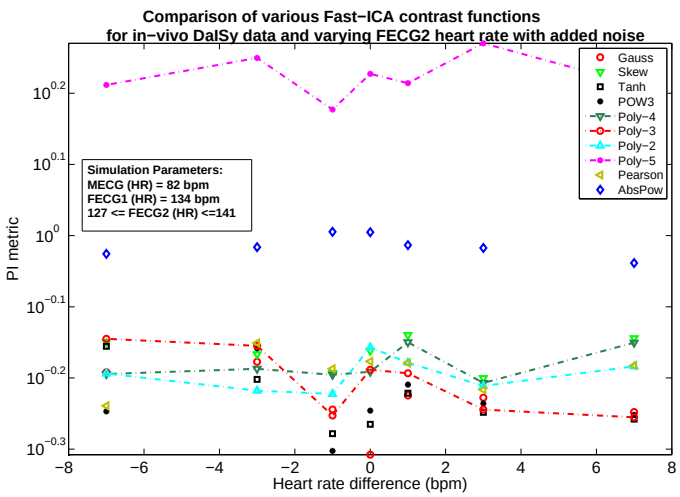

Fig. 12. PI metric for the data-centric schemes (Poly-L) and AbsPow compared with standard Fast-ICA schemes for in-vivo DaISy data-base with varying FECG2 heart rate and with Gaussian and EMG noise added.

TABLE IV
MEAN PI METRIC FOR RECONSTRUCTING ABIO7 DATASET

ICA Contrast Function	PI metric
Gauss	0.73
Skew	1.75
Tanh	0.77
Pow3	0.98
Poly-4	1.30
Poly-3	1.08
Poly-2	1.81
Poly-5	1.49
Pearson	2.51
AbsPow	0.87

centric *AbsPow* performed really well almost on-par with the *Gauss* contrast function. The other *Poly-L* methods were worse in their performance (Table IV). The reconstruction of the ABio7 data-set using *AbsPow* is also shown in Fig 13, which shows a clean reconstruction.

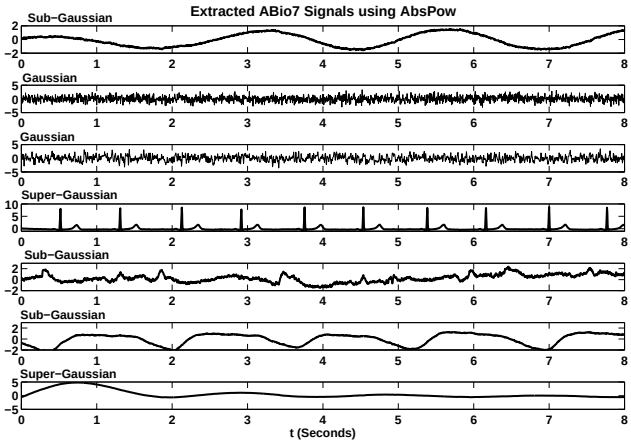

Fig. 13. Reconstruction of the ABio7 data-set using AbsPow

We also finally compared the computation speed of these algorithms for 1 trial, independent of fitting of the pdf functions and Table V shows the times in milli-seconds.

TABLE V
ALGORITHM SEPARATION TIME FOR ALL ICA SCHEMES

ICA Contrast Function	Computation Time (ms)
Gauss	88
Skew	57
Tanh	90
POW3	133
Poly-4	520
Poly-3	325
Poly-2	207
Poly-5	725
Pearson	197
AbsPow	137

The data-centric schemes are slightly more intensive in computation time as expected but AbsPow shows the least burden in this comparison.

IV. CONCLUSIONS

In this study, we investigated Fast-ICA algorithm to extract simulated twin FECG from abdominal ECG channel data under different types of interference for purposes of twin fetal health assessment. The performance of Fast-ICA algorithm is shown to improve via choice of contrast functions which is highly data dependent. We explored various contrast functions including the standard ones such as *tanh, gauss, skew, pow3*, and well-known *pearson* contrast function. Furthermore, we proposed new polynomial based contrast functions, *poly-L*, in which the coefficients of the polynomial are obtained from the empirical pdf of the data and *abspow* in which the order is selected experimentally. Our approach is based on modifying certain parameters of the contrast function using extracted features of the data.

We show a variety of simulations including simulated data sets, real in-vivo data from DaISy dataset, and ABio7 from ICALAB. We quantify reconstruction performance using a PI metric that is scale and order independent. In the case of ECG signal extraction, new data-centric contrast functions (*Poly-3* and *AbsPow*) are shown to be superior to the data based *Pearson* method and works on par and in some cases better than standard ICA polynomial schemes like *Skew*, *Pow3*. PI metrics for contrast functions with order $3-4$ (*Poly-3*, *Pow3*, *AbsPow* with $\alpha = 3$, offered in many cases, the lowest or best performance contrary to the fact that contrast functions which grow faster than $|y|$ are unrobust and, hence leads to low performance. This supports the need for data-centric contrast functions if one wants to optimize the performance of Fast-ICA. On the other hand, robust contrast functions *tanh* and *gauss* perform considerably better than *pearson* in both ECG extraction and for the general data set Abio7. We have also showed that the performance gain of the proposed polynomial-based schemes do increase the complexity, but not considerably.

Overall, this work does not only propose new techniques, but also provides an in depth comparison among the existing Fast-ICA techniques in the literature for ECG signal in the context for twin pregnancy data.

REFERENCES

[1] M. J. Lewis, "Review of electromagnetic source investigations of the fetal heart," *Medical Engineering and Physics*, vol. 25, pp. 801–810, 2003.

[2] M. O. Bahtiyar, A. T. Dulay, B. P. Weeks, A. H. Friedman, and J. A. Copel, "Prevalence of congenital heart defects in monochorionic/diamniotic twin gestations," *Journal Ultrasound in Medicine*, vol. 26, pp. 1491–1498, 2007.

[3] S. Comani, D. Mantini, G. Alleva, E. Gabriele, M. Liberati, and G. L. Romani, "Simultaneous monitoring of separate fetal magnetocardiographic signals in twin pregnancy," *Journal Ultrasound in Medicine*, vol. 26, pp. 193–201, 2005.

[4] C. Kahler, E. Schleubner, B. Grimm, U. Schneider, J. Haueisen, L. Vogt, and H. Seewald, "Fetal magnetocardiography in the investigation of congenital heart defects," *Early Human Development*, vol. 69, pp. 65–75, 2002.

[5] S. M. Martens, C. Rabotti, M. Mischi, and R. J. Sluijter, "A robust fetal ECG detection method for abdominal recordings," *Physiological Measurement*, vol. 28, pp. 373–388, 2007.

[6] L. K. Hornberger and D. J. Sahn, "Rhythm abnormalities of the fetus," *Heart*, vol. 93, pp. 1294–1300, 2007.

[7] P. Comon and C. Jutten, *Handbook of Blind Source Separation, Independent Component Analysis and Applications*, 1st ed. Academic Press, 2009.

[8] L. D. Lathauwer, B. Moor, and J. Vandewalle, "Fetal electrocardiogram extraction by blind source subspace separation," *IEEE Transactions on Biomedical Engineering*, vol. 47, no. 5, pp. 567–572, 2000.

[9] A. Gupta, M. C. Srivastava, V. Khandelwal, and A. Gupta, "A novel approach to fetal ECG extraction and enhancement using blind source separation (BSS-ICA) and adaptive fetal ecg enhancer (AFE)," in *IEEE ICICS*, 2007, pp. 983–987.

[10] B. Widrow, J. Glover, J. Mccool, J. Kaunitz, C. Williams, H. Hearn, and R. Googlin, "Adaptive noise cancelling: principles and applications," in *IEEE Proceedings*, 1975, pp. 1692–1716.

[11] A. Kam and A. Cohen, "Detection of fetal ECG with IIR adaptive filtering and genetic algorithms," in *Proc. ICASSP*, 1999, pp. 2335–2338.

[12] P. P. Kanjilal, P. Sarbani, and S. Goutam, "Fetal ECG extraction using singular value decomposition," *IEEE Transactions Biomedical Engineering*, vol. 44, no. 1, pp. 51–59, 1997.

[13] C. Sanchez, J. Millet, J. Rieta, F. Castells, J. Rodenas, R. Ruiz, and V. Ruiz, "Packet wavelet decomposition: An approach for atrial activity extraction," *IEEE Computers in Cardiology*, vol. 29, pp. 33–36, 2002.

[14] V. Zarzoso and A. K. Nandi, "Noninvasive fetal electrocardiogram extraction: blind separation versus adaptive noise cancellation," *IEEE Transactions in Biomedical Engineering*, vol. 48, pp. 12–18, 2001.

[15] Y. Ye, Z. Zhang, J. Zeng, and L. Peng, "A fast and adaptive ICA algorithm with its application to fetal electrocardiogram extraction," *Signal Processing*, vol. 205, pp. 799–806, 2008.

[16] M. J. Taylor, M. J. Smith, M. Thomas, A. R. Green, F. Cheng, S. Oseku-Afful, L. Y. Wee, N. M. Fisk, and H. M. Gardiner, "Non-invasive fetal electrocardiography in singleton and multiple pregnancies," *British Journal Obstetric Gynaecology*, vol. 110, pp. 668–678, 2003.

[17] M. Burghoff and P. Van Leeuwen, "Separation of fetal and maternal magnetocardiographic signals in twin pregnancy using independent component analysis (ICA)," *Neurology and Clinical neurophysiology*, vol. 39, pp. 1–4, 2004.

[18] T. W. Lee, M. Girolami, and T. J. Sejnowski, "Independent component analysis using an extended infomax algorithm for mixed sub-gaussian and super-gaussian sources," *Neural Computation*, vol. 48, pp. 417–441, 1999.

[19] A. Hyvarinen, "Fast and robust fixed-point algorithms for independent component analysis," *IEEE Transactions On Neural Networks*, vol. 10, pp. 626–634, 1999.

[20] A. Hyvarinen, J. Karhunen, and P. Oja, *Independent component analysis*. Wiley interscience, 2001.

[21] J. Karvanen and V. Koivunen, "Blind separation methods based on pearson system and its extensions," *Signal Processing*, vol. 82, pp. 663–67, 2002.

[22] M. Keralapura, M. Pourfathi, and B. Sirkeci-Mergen, "Independent component analysis with data-centric contrast functions for separating maternal and twin fetal ECG," in *Lecture Notes in Engineering and Computer Science: Proceedings of WCECS*, 2010, pp. 857–862.

[23] J. Shao, *Mathematical Statistics*. Springer-Verlay New York, Inc, 1999.

[24] P. Huber, "Projection pursuit," *The Annals of Statistics*, vol. 13, no. 2, pp. 435–475, 1985.

[25] J. F. Cardoso, "Infomax and maximum likelihood for source separation," *IEEE Letters on Signal Processing*, vol. 4, pp. 112–114, 1997.

[26] ——, "Entropic contrasts for source separation," *in Adaptive Unsupervised Learning (editor: S. Haykin)*, vol. 1, pp. 139–190, 1999.

[27] A. J. Bell and T. J. Sejnowski, "An information-maximization approach to blind separation and blind deconvolution," *Neural Computation*, vol. 7, pp. 1129–1159, 1995.

[28] A. Mahajan and G. Birajdar, "Blind source separaation using modified contrast function in fast ica algorithm," *International Journal of Computer Applications*, vol. 6, no. 4, 2010.

[29] V. Ananthashayana and M. Jyothirmayi, "Blind source separation using modified gaussian Fast-ICA," in *World Academy of Science, Engineering and Technology*, vol. 56, 2009.

[30] J. Karvanen, J. Eriksson, and K. V., "Pearson system based method for blind separation," in *Proceedings of the Second International Workshop on Independent Component Analysis and Blind Signal Separation (ICA 2000). Helsinki, Finland*, 2000, pp. 585–590.

[31] H. Liang, "Adaptive independent component analysis of multichannel electrogastrograms," *Elsevier Medical Engineering & Physics*, vol. 23, pp. 91–97, 2001.

[32] P. E. McSharry, G. D. Clifford, J. Tarassenko, and L. A. Smith, "Dynamical model for generating synthetic electrocardiogram signals," *Signal Processing*, vol. 50, no. 3, pp. 289–294, 2003.

[33] B. D. Moor, P. D. Gersem, B. D. Schutter, and W. Favoreel, "DAISY: A database for identification of systems," *Special Issue on CACSD*, vol. 38, no. 3, pp. 4–5, 1997.

[34] A. Cichocki, S. Amari, K. Siwek, T. Tanaka, and A. H. Phan, *ICALAB Toolboxes*. http://www.bsp.brain.riken.jp/ICALAB, 2003.

[35] R. A. Shepovalnikov, A. P. Nemirko, A. N. Kalinichenko, and V. V. Abramchenko, "Investigation of time, amplitude, and frequency parameters of a direct fetal ECG signal during labor and delivery," *Pattern Recognition and Image Analysis*, vol. 16, no. 1, pp. 74–76, 2006.

[36] I. Sahin, N. Yilmazer, and M. A. Simaan, "A method for sub-sample fetal heart rate estimation under noisy conditions," *IEEE Transactions on Biomedical Engineering*, vol. 57, no. 4, pp. 875–883, 2010.

[37] A. L. Goldberger, L. A. N. Amaral, L. Glass, J. M. Hausdorff, P. C. Ivanov, R. G. Mark, J. E. Mietus, G. B. Moody, C. K. Peng, and H. E. Stanley, "Physiobank, physiotoolkit, and physionet: Components of a new research resource for complex physiologic signals," *Circulation*, vol. 101, no. 23, pp. e215–e220, 2000.